

# Output Perfect Tracking Control for a Plant with PWM-Type Input <sup>\*</sup>

Kohta Tamekuni <sup>\*</sup> Masayasu Suzuki <sup>\*</sup> Mitsuo Hirata <sup>\*</sup>

<sup>\*</sup> *Utsunomiya University, 7-1-2 Yoto, Utsunomiya, Tochigi 321-8585  
Japan (e-mail: tamekunikohta@tutanota.com,  
ma-suzuki@cc.utsunomiya-u.ac.jp, hirata@cc.utsunomiya-u.ac.jp).*

---

**Abstract:** It is a well-established fact that an unstable zero may appear when a minimum-phase continuous-time system is discretized by a zero-order hold. Therefore, a feedforward controller cannot be obtained based on the inverse system; this is because it becomes unstable. Herein, an exact linearization method for a continuous-time system with a pulse-width modulation-type (PWM-type) input has been proposed showing that unstable zeros of the linearized discrete-time system can be moved to the stable region by altering the pulse-centers location. This enables the construction of a stable feedforward controller that achieves an output perfect tracking control. However, the current paper shows a trade-off between the stability of the stabilized zero and the maximum pulse-width. This prevents the unstable zero from moving to a high stability region, and shows some oscillation at the output of the feedforward controller. To address this, a zero-phase error filter has been introduced to reduce the oscillation. Further, a nonlinear deadbeat controller is also proposed, which can be applied to second and higher order systems. The effectiveness of the proposed methods are presented in this paper by performing simulations.

*Keywords:* Pulse-width modulation, Perfect tracking control, Discrete-time unstable zeros, Feedforward control

---

## 1. INTRODUCTION

A controller that computes the controlling input for tracking with a zero error on sampling instants is classified as a perfect tracking controller (PTC) (see (Tomizuka, 1987)). For a given discrete-time plant model  $P$ , if the zeros of  $P$  are stable, a simple approach to achieve a PTC is to use the inverse model and employ a feedforward (FF) controller  $z^{-d}/P(z)$ ; wherein,  $d$  is the relative degree of  $P$ . However, discrete-time models have the possibility of possessing unstable zeros even if the original continuous-time plants do not (see (Åström et al., 1984)). Although the double integrator system  $1/s^2$  is frequently involved in the motion control field, its zero-order-hold (ZOH) discretized model has an unstable zero at  $z = -1$ ; this is regardless of sampling rate. Furthermore, the behavior of the double integrator system with a pulse-width modulation (PWM) input, in which each pulse is located at the center of the control interval, coincides with the ZOH model on the sampling instants. Hence, the inverse of the plant cannot be used.

The zero-phase error tracking controller (ZPETC) proposed by Tomizuka (1987) is a FF controller that cancels all of the poles and stable zeros of the plant, and compensates for the phase characteristics arising from the unstable zeros. There is no phase error from the reference to the output when applying the ZPETC. However, the tracking error cannot be eliminated completely in the high-frequency region because the high-frequency gain is less

than 0 dB. In contrast, Wen and Potsaid (2004) proposed zero-magnitude error controller (ZMETC), which guarantees that gain is equal to unity at every frequency, but there are phase errors instead. Meanwhile, Fujimoto et al. (2001) have succeeded in the perfect tracking by constructing a multi-sampling rate control system. However, this method requires preparing reference orbits for whole state variables.

In this paper, a novel FF controller for the double integrator system with the PWM-type input is used to achieve the output PTC, which only requires output references. The authors have proposed an exact linearization<sup>1</sup> method for continuous-time systems with the PWM-type input in (Suzuki et al., 2019). Based on (Suzuki et al., 2019), it can be shown that the zero of the linearized discrete-time double integrator system can be moved to the stable region by fixing the center of the pulse to the first half part of the control interval. This enables the construction of a stable FF controller for achieving the output PTC.

However, because there is a trade-off between the stability degree of the zero and the maximum pulse-width, the unstable zero cannot be moved to a high stability region; this results in some oscillation at the output of the FF controller. For this problem, we employ a model matching control with a zero-phase error filter to reduce the oscillation. Further, we also propose a nonlinear output deadbeat controller in which the pulse-center is no longer fixed and there is no restriction for the pulse-width. The output

---

<sup>\*</sup> This work was partially supported by JSPS KAKENHI Grant Numbers JP19K04438 and JP17K14698 .

---

<sup>1</sup> In general, PWM-type input systems exhibit nonlinear behavior in terms of the pulse parameters, even on the sampling instants.

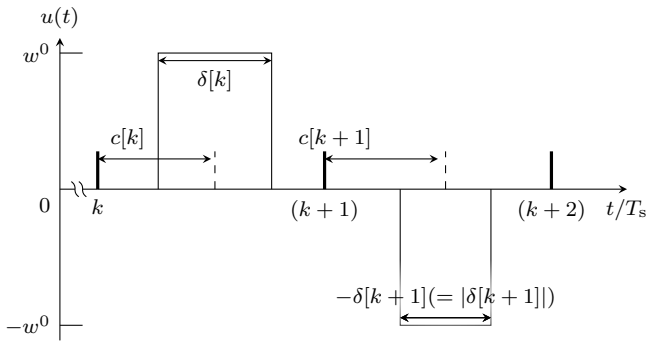


Fig. 1. Example of PWM-type input  $u(t)$ : Each pulse is determined by the pulse center  $c$  and pulse width  $\delta$ .

deadbeat approach can be used for not only a second-order system but also higher-order systems. A high-order continuous system is introduced by taking into account the turn-on/off dynamics of the pulses, to which the nonlinear deadbeat control is applied.

## 2. DOUBLE INTEGRATOR WITH PWM-TYPE INPUT

### 2.1 Problem formulation

Consider the following double integrator system  $(A_c, B_c, C)$  with scalar-valued input  $u$  and output  $y$ :

$$\dot{x}(t) = \begin{bmatrix} 0 & 1 \\ 0 & 0 \end{bmatrix} x(t) + \begin{bmatrix} 0 \\ 1 \end{bmatrix} u(t), \quad (1a)$$

$$x(0) = [0, 0]^T, \quad (1b)$$

$$y(t) = [1 \ 0] x(t). \quad (1c)$$

The input  $u$  is given as a sequence of positive/negative pulses whose heights are  $w^0 (> 0)/-w^0$ , respectively. At most one pulse is located in each control interval of period  $T_s$ . The width and center of each pulse in the  $k$ th control interval are denoted by  $\delta[k] \in [-1, 1]$  and  $c[k] \in [0, 1]$ , respectively, where  $\delta[k] < 0$  means that the pulse is negative. Therefore,  $u$  can be represented as follows (see also Fig. 1):

$$u(t) = \begin{cases} w^0 \text{sgn}(\delta[k]), & t/T_s - k \in \Delta[k], \\ 0, & \text{otherwise,} \end{cases} \quad (2a)$$

$$\Delta[k] := \left[ c[k] - \frac{|\delta[k]|}{2}, c[k] + \frac{|\delta[k]|}{2} \right] \subset [0, 1]. \quad (2b)$$

Let  $r[k], k = 1, 2, \dots$ , be the reference signal for the output  $y$ . The objective is to design a control system that achieves the perfect tracking of the output  $y$  for reference  $r$ . To this end, we employ a two-degree-of-freedom controller as shown in Fig. 2. While the feedback (FB) controller is assigned to compensate modeling errors and to suppress disturbances, the feedforward (FF) controller plays a significant role in improving the tracking response.

This present paper focuses on the FF design aspects such as, the cascade system of the FF controller, pulse generator, plant, and sampler. This paper will also address an issue of determining the pulse generating rule (i.e.,  $c$  and  $\delta$  in (2)).

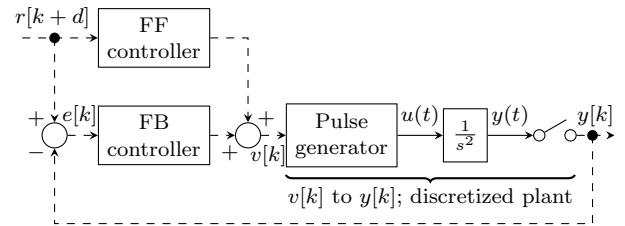


Fig. 2. Two-degree-of-freedom control system.

### 2.2 Behavior on sampling instants

The behavior of (1) with the PWM-type input of (2) on sampling instants is governed by the following discrete-time equations:

$$x[k+1] = Ax[k] + I(c[k], \delta[k]), \quad (3a)$$

$$y[k] = Cx[k], \quad (3b)$$

where

$$A := \exp(A_c T_s), \quad (4a)$$

$$\begin{aligned} I(c, \delta) &:= w^0 \int_{T_s(c-\delta/2)}^{T_s(c+\delta/2)} e^{A_c(T_s-\tau)} B_c d\tau \\ &= w^0 \begin{bmatrix} T_s^2(1-c) \\ T_s \end{bmatrix} \delta. \end{aligned} \quad (4b)$$

Note that the mapping  $I$  includes the product of  $c$  and  $\delta$ . Therefore, if  $c[k]$  and  $\delta[k]$  are manipulated simultaneously, the vector  $I(c[k], \delta[k])$  changes in a nonlinear fashion.

Here, the center  $c[k]$  is fixed to some value  $c^* \in (0, 1)$ . Then,  $I(c^*, \cdot)$  is defined on  $[-\delta_{\max}, \delta_{\max}]$ ,  $\delta_{\max} = \min\{2c^*, 2(1-c^*)\}$ , and  $I(c^*, \delta)$  behaves linearly with respect to  $\delta$  if  $\delta$  belongs within the domain. This mapping is denoted by

$$I(c^*, \delta) = B_{c^*} \delta, \quad \delta \in [-\delta_{\max}, \delta_{\max}], \quad (5)$$

where  $B_{c^*} := w^0 [T_s^2(1-c^*) \ T_s]^T$ . Because the response of (1) on sampling instants obeys

$$x[k+1] = Ax[k] + B_{c^*} \delta[k], \quad (6a)$$

$$y[k] = Cx[k], \quad (6b)$$

the transfer function from  $\delta[k]$  to  $y[k]$  can be calculated as

$$\begin{aligned} P_{c^*}(z) &= C(zE - A)^{-1} B_{c^*} \\ &= \frac{w^0 T_s^2 (1-c^*) \{z + c^*/(1-c^*)\}}{(z-1)^2}, \end{aligned} \quad (7)$$

where  $E$  is the identity matrix.

From (7), it turns out that the zero of  $P_{c^*}(z)$  is

$$-\frac{c^*}{1-c^*} (= z_0), \quad (8)$$

and is determined by the pulse-center  $c^*$ . When  $c^* = 0.5$ , the zero becomes marginally stable ( $z_0 = -1$ ): In fact, (7) with  $c^* = 0.5$  coincides with the zero-order-hold discretized model of (1). If one sets the center as  $c^* > 0.5$ , the zero becomes unstable ( $z_0 < -1$ ). Conversely, when  $c^* < 0.5$ ,  $z_0$  is stable ( $-1 < z_0 < 0$ ). More specifically, the stability degree of  $z_0$  increases as  $c^*$  decreases from 0.5 to 0. Thus, the zero can be moved by changing the pulse location. This property is also observed for systems other than the double integrator system (Suzuki et al., 2019), and is interesting because the zeros cannot be adjusted by FB control in general.

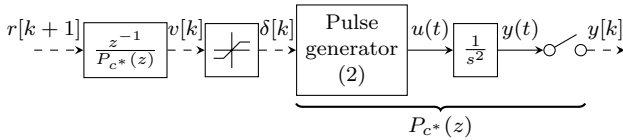


Fig. 3. Perfect tracking control using inverse model.

### 3. TRACKING CONTROL USING INVERSE MODELS

#### 3.1 Perfect tracking control using stable inverse models

By fixing the center of the pulse to the first half part of the control interval, the zero of the discrete-time system (6) can be moved to the stable region. This enables us to prepare a stable inverse model, and construct a FF controller  $z^{-1}/P_{c^*}(z)$  as shown in Fig. 3. The saturation block in Fig. 3 is assigned to restrict pulse-width, which is defined by the following:

$$\delta[k] = \begin{cases} v[k], & |v[k]| \leq \delta_{\max}, \\ \delta_{\max} \text{sgn}(v[k]), & |v[k]| > \delta_{\max}, \end{cases} \quad (9)$$

where  $v$  is the output of the FF controller.

In deriving the above FF controller, any approximation is not performed. The discrete-time model  $P_{c^*}(z)$  completely captures the behavior of the plant, and allows the FF controller to achieve the output perfect tracking as long as the relation  $|v[k]| \leq \delta_{\max}$  is satisfied.

The top figure in Fig. 4 shows the time-response of the system in Fig. 3, where the pulse-center is fixed at  $c^* = 0.4$  and the simulation was performed under the conditions in Table 1. This result includes the intersample response/error (solid-line/dot-line) as well as the response/error on the sampling instants (circles/squares). It turns out from the top figure that the output  $y$  perfectly agrees with the reference on the sampling instants, that is,  $y[k] = r[k]$ . The bottom figure in Fig. 4 shows the time-series of  $v$ . Because the FF controller is stable,  $v[k]$  does not excessively oscillate or diverge. However, the sign of  $v[k]$ , corresponding to the sign of the pulse, changes each step during the transient period of  $k < 5$ . This large fluctuation can be considered to affect the intersample behavior.

Fig. 5 depicts the signals of  $v$  for the cases of  $c^* = 0.2, 0.3$  and  $0.4$ . In the transient period, the smaller value of  $c^*$  correlates to a smaller value of the variation of  $v$ . This occurs because the FF controller becomes more stable by choosing a smaller  $c^*$ , and the small variation of  $v$  seems to be worthwhile at a glance. However, when  $c^* = 0.2$ ,  $v[0]$  actually exceeds  $\delta_{\max} = 0.4$ , and hence, the pulse-width is shortened to  $\delta_{\max} T_s$ , which implies that the perfect tracking is not achieved. These results show that there exists a trade-off between the stability degree of the stabilized zero and the maximum pulse-width. The unstable zero cannot be moved to a high stability region,

Table 1. Simulation parameters

Sampling period $T_s$	1
Reference $r[k] = r(kT_s)$	$r(t) = \begin{cases} 0 & (t < 0) \\ \sin(2\pi/(10T_s)t) & (t \geq 0) \end{cases}$
Pulse height $w^0$	1.5

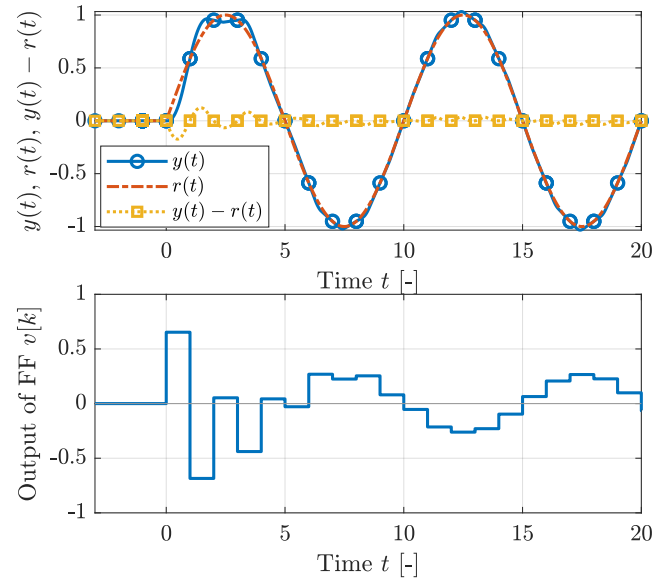


Fig. 4. Tracking response for PTC using the inverse model: The pulse-center is fixed at  $c^* = 0.4$ .

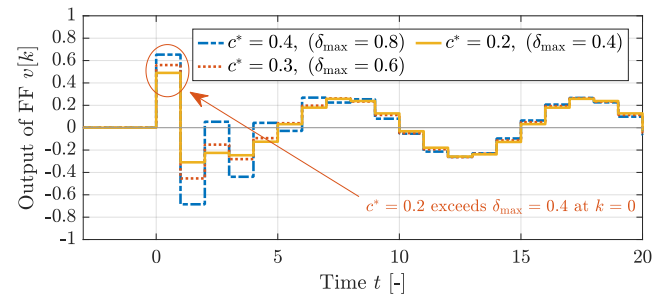


Fig. 5. Control input for PTC by inverse model: As decreasing  $c^*$ , decreasing oscillation. However, a control input exceeds  $\delta_{\max}$

and this results in some oscillation at the output of the FF controller.

#### 3.2 Zero phase error tracking control using stable inverse models

We have confirmed that the inverse model  $1/P_{c^*}$  is stable when  $c^* < 0.5$ , but one cannot choose an arbitrarily small  $c^*$  due to pulse-width limitations. While the zero can be stabilized, it may lie near the unit circle. This leads to produce large variations in the output of the FF controller.

Consider the model-matching control as shown in Fig. 6 for an arbitrary stable reference model  $M(z)$  and a stable  $1/P_{c^*}$ . Parameter  $d$  in Fig. 6 is for making the FF controller be proper. The transfer function from the reference to the output is  $z^{-d}M(z)$ , and hence, the response of  $M(z)$  can be derived by giving a  $d$ -step-forward reference signal  $r[k+d]$ . Note that the FF controller in Fig. 3 is a special version of Fig. 6 with  $M(z) = 1$  and  $d = 1$ . It is trivial that the model  $M(z) = 1$  has flat gain and phase characteristics for all frequencies.

The following reference model is used:

$$M(z) = \frac{1}{(1-\xi)^2} (z-\xi)(z^{-1}-\xi), \quad (10)$$

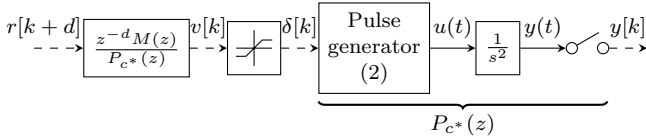


Fig. 6. Model matching control

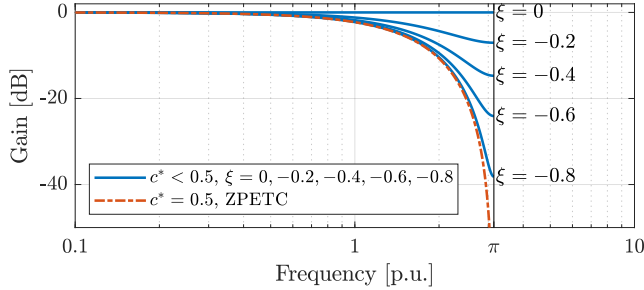


Fig. 7. Gain plot of the transfer function from the reference  $r[k]$  to the output  $y[k]$ : The blue solid-lines depict the gain characteristics of (10), and the red dashed-line depicts that of (15)  $\times z^2$  by ZPETC.

where  $\xi \in [-1, 0]$  is a tuning parameter. We have

$$M(e^{j\omega}) = \frac{(e^{j\omega} - \xi)(e^{j\omega} - \bar{\xi})}{(1 - \xi)^2} \in \mathbb{R}. \quad (11)$$

Because the imaginary part of  $M(e^{j\omega})$  is always 0, it turns out that the phase shift of (10) is zero for all frequencies. For the model (10), the FF controller becomes

$$G_{\text{FF}}(z) = \frac{z^{-2}M(z)}{P_{c^*}(z)} = \frac{(z - \xi)z^{-2}(z^{-1} - \bar{\xi})(z - 1)^2}{z - z_0 w^0 T_s^2 (1 - c^*)(1 - \xi)^2}. \quad (12)$$

Approximate cancellation of the pole  $z_0$  and zero  $\xi$  is expected to decrease variation caused by the zero  $z_0$  near the unit circle.

Meanwhile, zero-phase error tracking control (ZPETC) by Tomizuka (1987) has been well-established as a design method for FF controllers that achieves zero phase shift for plants with unstable zeros.

When a conventional center-located pulse is employed, the discrete-time transfer function becomes

$$P_{0.5}(z) = \frac{w^0 T_s^2 (z + 1)}{2(z - 1)^2}. \quad (13)$$

According to the ZPETC theory by Tomizuka (1987), we derive the following FF controller:

$$G_{\text{FF}}^{\text{ZPETC}}(z) = \frac{(z - 1)^2 (z + 1)}{2w^0 T_s^2 z^3}. \quad (14)$$

Subsequently, the transfer characteristic from  $r[k + 2]$  to  $y[k]$  is

$$\frac{(z + 1)^2}{4z^3}. \quad (15)$$

Gain characteristics from the reference  $r[k]$  to the output  $y[k]$  for both the proposed FF and conventional ZPETC system are depicted in Fig. 7. This figure shows that the proposed FF method is superior when comparing gain error.

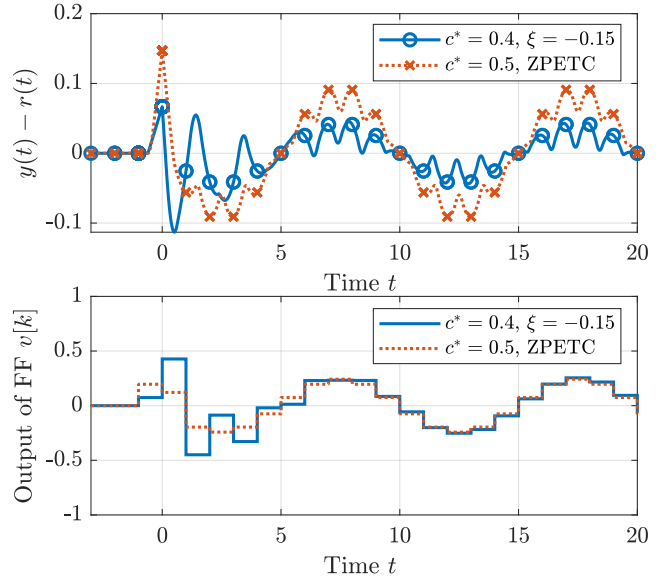


Fig. 8. Tracking errors: For the proposed method, the design parameters are chosen as  $c^* = 0.4$  and  $\xi = -0.15$ .

Furthermore, the proposed method still exhibits a degree-of-freedom in selecting the parameter  $\xi$ . The  $\xi$  parameter is tuned to an appropriate value when the balance between the gain error and the oscillation of the FF controller is considered. Because  $M(z)$  approaches 1 as  $\xi$  increases to 0, the gain error can be suppressed by choosing a large  $\xi$ . However, in this case,  $\xi$  and the pole near the unit circle are not close enough to be approximately canceled out; this causes oscillation of the FF controller. Alternatively, if  $\xi$  is chosen around  $z_0$ , the variation in the output of the FF controller will be small, while the gain error may be significant.

Fig. 8 shows a simulation result for the condition of Table 1, where  $c^* = 0.4$  and  $\xi = -0.15$  for the proposed method. The top figure in Fig. 8 depicts the errors  $y(t) - r(t)$ . Results show that the proposed method suppresses the error better than the conventional ZPETC. The bottom figure in Fig. 8 shows the output of the FF controllers. Although the variation of the proposed method is larger as compared to the conventional ZPETC, it is smaller when compared to the result of Fig. 4 in Sec. 3.1.

#### 4. NONLINEAR OUTPUT DEADBEAT CONTROL

In the previous section, the discrete-time dynamics obey a linear model with a stable zero; this is observed when the pulse-center is fixed at some suitable position. As such, we have designed FF controllers using its inverse model. However, because the zero cannot be moved to a high stability region, the output of the FF controller may exhibit oscillation. For this concern, a zero-phase error filter is introduced in one direction to reduce the oscillation. A nonlinear FF controller is proposed as an alternative method to reduce oscillation. This approach manipulates both the pulse-width and the location of the pulse-center at every control period.

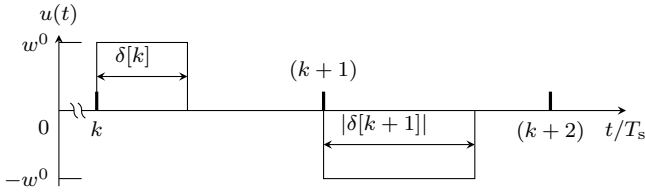


Fig. 9. Example of leading-edge-fixed pulses.

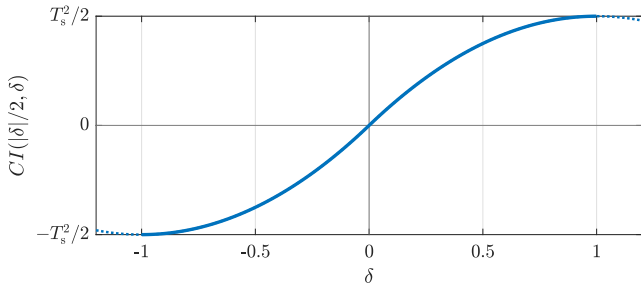


Fig. 10. The function  $CI(|\delta|/2, \delta)$ .

#### 4.1 Nonlinear output deadbeat control for the double integrator system

In Suzuki and Hirata (2018), the solvability of an output deadbeat control problem for multi-degree-of-freedom PWM-input systems is discussed. Based on this idea, the following nonlinear equation for the discrete-time model (3) is considered:

$$CI(c[k], \delta[k]) = r[k+1] - CAx[k]. \quad (16)$$

If  $c[k]$  and  $\delta[k]$  are successively found for the current state  $x[k]$  and a given reference  $r[k+1]$ , the output PTC can be achieved.

Eq. (16) is underdetermined because two parameters exist for one scalar equation. We here fix the leading edges of pulses at 0 (see Fig. 9), which implies that the pulse-center  $c[k]$  varies depending on the pulse-width  $\delta[k]$ :

$$c[k] = |\delta[k]|/2. \quad (17)$$

This is motivated by the fact observed in Sec. 2.2; the more the pulse-center is moved to the left, the more stable the discrete-time zero of  $P_{c^*}$  becomes. Although the equation (16) with (17) is still nonlinear, the mapping  $CI(|\delta|/2, \delta)$  is a monotone function on  $[-1, 1]$  as shown in Fig. 10. Therefore, the inverse problem can be easily solved. It should be emphasized that the pulse-width is no longer restricted to some subinterval using this approach.

Fig. 11 shows the block diagram implementing the nonlinear deadbeat law. Although (16) includes the state value  $x[k]$ , this vector is not the actual state of the plant. It is simulated in the FF controller that only requires the actual initial state  $x[0]$ . Fig. 12 shows a simulation result under the condition of Table 1. Comparing to Fig. 4, where the pulse-center is fixed at  $c^* = 0.4$  and PTC is applied using the inverse model, the variation of the duty ratio decreases and the intersample response improves.

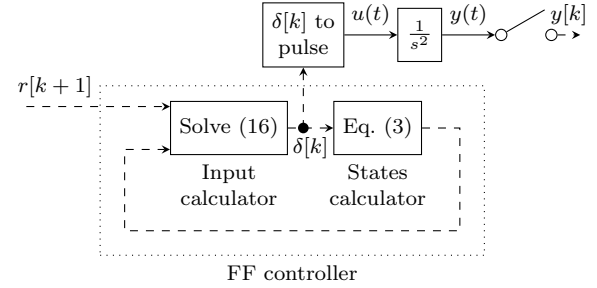


Fig. 11. FF control system using a nonlinear deadbeat approach for the double integrator.

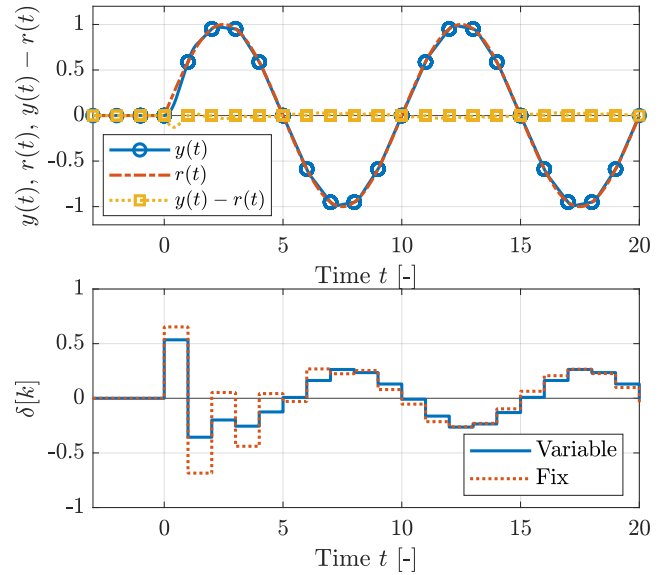


Fig. 12. Tracking response of the FF control system in Fig. 11. The red dotted line in the bottom figure depicts the pulse-width when the pulse-center is fixed at  $c^* = 0.4$  and the PTC in Sec. 3.1 is applied.

#### 4.2 Application to high-order systems: Compensation of switching characteristic

Output perfect tracking controllers based on the nonlinear deadbeat are designed for not only a second order system but also higher-order systems.

As PWM-type inputs to the double integrator system, ideal switching responses were considered so far. It was assumed that the turn-on and -off of the control inputs occur instantaneously. However, they have necessarily time lags in practice. To take into account practical switching responses, the following linear filter is assigned in front of the double integrator as shown in Fig. 13:

$$P_{Ce}(s) = \frac{\omega_n^2}{s^2 + 2\zeta\omega_n s + \omega_n^2}. \quad (18)$$

The parameters  $\zeta$  and  $\omega_n$  are chosen so that  $P_{sw}(s)$  becomes the second-order Butterworth filter whose peak time is  $T_s/20$ . Fig. 14 shows a filtered switching response  $u_{sw}$ .

The continuous-time plant is a fourth-order system. Similar to a second-order system, a discrete-time model corresponding to (3) can be calculated. Then, by solving the problem (16) with (17), the pulse-width is determined.

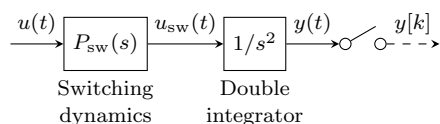


Fig. 13. Block diagram for a double integrator with switching dynamics

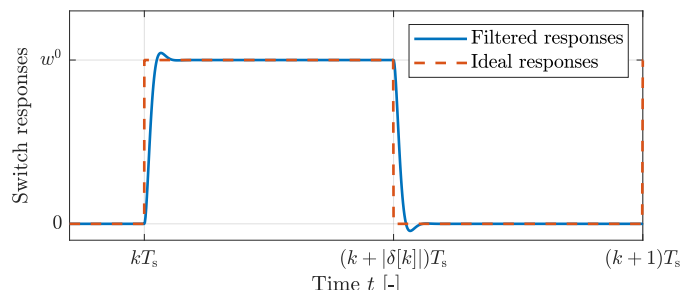


Fig. 14. Ideal and practical switching responses.

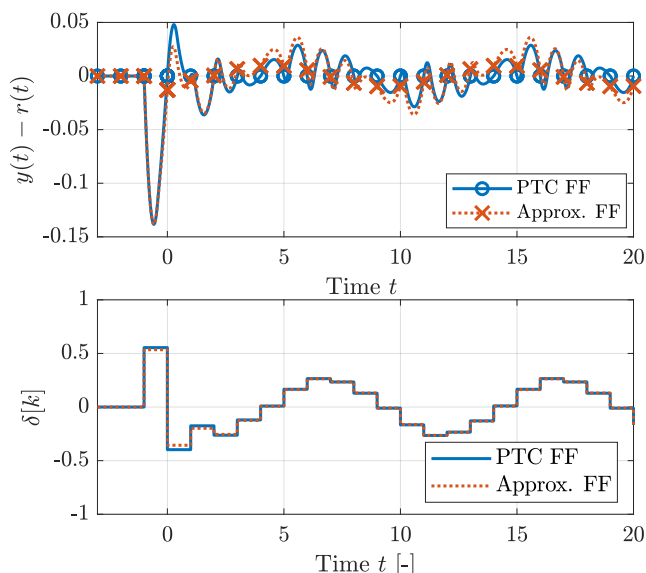


Fig. 15. Simulation results for the plant in Fig.13. The red dotted line depicts a simulation result in which the switching dynamics  $P_{sw}(s)$  is not taken into account. The blue solid line depicts a simulation result in which the switching dynamics is considered.

Under the condition of Table 1, two simulations have been performed. One simulation does not take into account the switching dynamics  $P_{sw}(s)$  (that is, the same pulse-widths as Fig. 12 are applied), and the other simulation does. In both simulations, the control object is the fourth-order system  $P_{sw}(s)P(s)$ . Fig. 15 shows the simulation results. When the switching dynamics are ignored, errors exist at sampling instants. Meanwhile, the output PTC has been achieved when the switching dynamics is taken into account.

## 5. CONCLUSIONS

In this paper, for a continuous-time double integrator system with a PWM-type input, it has been shown that unstable zeros of the linearized discrete-time system can be transferred to the stable region by fixing the center of

the pulse to the first half part of the control interval. This enables us to construct a stable feedforward controller for achieving an output PTC.

However, a trade-off occurs between the stability degree of the zero and the maximum pulse-width. Therefore, the unstable zero cannot be moved to a high stability region; this leads to the occurrence of some oscillation. To address this, a zero-phase error filter is introduced to reduce oscillation. Additionally, a nonlinear FF controller is proposed, which manipulates both the duty ratio and the location of the pulse-center at every control period. Herein, the output PTCs are based on the proposed method, are designed not only for a second order system but for a higher-order system. The effectiveness of the proposed methods have been shown by performing simulations.

## REFERENCES

- Åström, K., Hagander, P., and Sternby, J. (1984). Zeros of sampled systems. *Automatica*, 20(1), 31–38.
- Fujimoto, H., Hori, Y., and Kawamura, A. (2001). Perfect tracking control based on multirate feedforward control with generalized sampling periods. *IEEE Transactions on Industrial Electronics*, 48(3), 636–644.
- Suzuki, M. and Hirata, M. (2018). Partial state perfect tracking control of PWM-type input systems. In *Proc. of International Symposium on Nonlinear Theory and Its Applications*, 124–127.
- Suzuki, M., Tamekuni, K., and Hirata, M. (2019). A remark on zero placement in exact linearization using multi-degree-of-freedom PWM-type input. In *Proc. of Asian Control Conference*, 1199–1204.
- Tomizuka, M. (1987). Zero phase error tracking algorithm for digital control. *Journal of Dynamic Systems, Measurement, and Control*, 109(1), 65–68.
- Wen, J.T. and Potsaid, B. (2004). An experimental study of a high performance motion control system. In *Proc. of American Control Conference*, 5158–5163.